Virus Research 272 (2019) 197732

Contents lists available at ScienceDirect

Virus Research

journal homepage: www.elsevier.com/locate/virusres

The use of green fluorescent protein-tagged virus-like particles as a tracer in the early phase of chikungunya infection

Uranan Tumkosit[a], Yusuke Maeda[b], Natsuko Kishishita[a,b,1], Uamporn Siripanyaphinyo[a], Hiroko Omori[b], Prukswan Chetanachan[c], Pathompong Sittisaman[c], Chaitas Jityam[c], Thongkoon Priengprom[a], Hiroto Mizushima[a,b], Pattara Wongjaroen[c], Eisuke Mekada[b], Masashi Tatsumi[b], Naokazu Takeda[b], Atsushi Tanaka[a,b,*]

[a] Thailand–Japan Research Collaboration Center on Emerging and Re-emerging Infections (RCC-ERI), Department of Medical Sciences, Ministry of Public Health, Nonthaburi, Thailand
[b] Research Institute for Microbial Diseases (RIMD), Osaka University, Suita, Osaka, Japan
[c] National Institute of Health, Department of Medical Sciences, Ministry of Public Health, Nonthaburi, Thailand

ARTICLE INFO

Keywords:
Chikungunya virus
Virus-like particle
EGFP
Internalization

ABSTRACT

To visually examine the early phase of chikungunya virus (CHIKV) infection in target cells, we constructed a virus-like particle (VLP) in which the envelope protein E1 is fused with green fluorescent protein (GFP). This chikungunya VLP-GFP (CHIK-VLP-EGFP), purified by density gradient fractionation, was observed as 60–70 nm-dia. particles and was detected as tiny puncta of fluorescence in the cells. CHIK-VLP-EGFP showed binding properties similar to those of the wild-type viruses. Most of the fluorescence signals that had bound on Vero cells disappeared within 30 min at 37 °C, but not in the presence of anti-CHIKV neutralizing serum or an endosomal acidification inhibitor (bafilomycin A1), suggesting that the loss of fluorescence signals is due to the disassembly of the viral envelope following the internalization of CHIK-VLP-EGFP. In addition to these results, the fluorescence signals disappeared in highly susceptible Vero and U251MG cells but not in poorly susceptible A549 cells. Thus, CHIK-VLP-EGFP is a useful tool to examine the effects of the CHIKV neutralizing antibodies and antiviral compounds that are effective in the entry phase of CHIKV.

1. Introduction

Chikungunya fever is a mosquito-borne disease that occurs mainly in tropical regions such as those in Africa, South Asia, and Southeast Asia (Burt et al., 2012), and it has recently spread to Europe and the Americas (Morrison, 2014; Parola et al., 2006; Weaver, 2014). This infectious disease is transmitted by the bite of certain species of mosquitoes infected with the chikungunya virus (CHIKV). Chikungunya fever usually begins 2–12 days after the bite and is characterized by the sudden onset of a high fever that is frequently accompanied by severe joint pain, muscle pain, headache, nausea, fatigue and rash. Individuals suffering from CHIKV show joint pain that usually lasts for a few days but may persist for several months or even years after the initial infection (Burt et al., 2012; Morrison, 2014; Pialoux et al., 2007; Weaver, 2014). Neurological complications of CHIKV infection including encephalitis, meningoencephalitis, peripheral neuropathies, and Guillain-Barré syndrome have been reported (Das et al., 2010; Economopoulou et al., 2009; Robin et al., 2008; Tournebize et al., 2009). Neither a specific antiviral drug for the treatment of the chikungunya fever nor a commercial vaccine for chikungunya fever is available. The treatment of joint pain due to Chikungunya fever is focused on relieving the symptoms with antipyretics, optimal analgesics, and fluids.

CHIKV is a member of the genus *Alphavirus* in the family *Togaviridae*. The genome of CHIKV is a positive-sense single-stranded RNA genome of 11.8 kb encoding four nonstructural and five structural proteins. The structural proteins are translated from a subgenomic 26S mRNA as a single polyprotein, which is processed co-translationally into five structural proteins: capsid, E3, E2, 6 K, and E1 (Leung et al., 2011). These structural proteins form two T = 4 quasi-icosahedral

* Corresponding author at: Thailand–Japan Research Collaboration Center on Emerging and Re-emerging Infections (RCC-ERI), Department of Medical Sciences, Ministry of Public Health, Nonthaburi, Thailand.
E-mail address: washi69@biken.osaka-u.ac.jp (A. Tanaka).
[1] Present address: Center for Drug Design Research, National Institutes of Biomedical Innovation, Health and Nutrition, Ibaraki, Osaka, Japan.

https://doi.org/10.1016/j.virusres.2019.197732
Received 6 June 2019; Received in revised form 13 August 2019; Accepted 20 August 2019
Available online 21 August 2019
0168-1702/

symmetry layers: the viral surface lipid membrane with a dia. of 65–70 nm containing 80 viral envelope spikes that consist of 240 copies of the E1-E2 heterodimer, and the icosahedral nucleocapsid core comprised of 240 copies of the capsid (Cheng et al., 1995; Jose et al., 2009; Simizu et al., 1984; Voss et al., 2010). Viral envelope E2 glycoprotein is responsible for the binding to the cell surface receptor, and E1 protein serves as a fusion protein (Boggs et al., 1989; Jose et al., 2009; Justman et al., 1993; Kielian and Helenius, 1985; Omar and Koblet, 1988; Sanz et al., 2003; Smith et al., 1995). (Zhang et al., 2018) reported that an adhesion molecule, Mxra8 is a receptor for arthritogenic alphaviruses, including chikungunya virus. Mxra8 enhanced CHIKV attachment and internalization into target cells regardless of whether the target cells expressed heparan sulfate, which is known as a primary attachment factors for various viruses including CHIKV (Ashbrook et al., 2014; Rostand and Esko, 1997; Silva et al., 2014; Tanaka et al., 2017). However, the availability of Mxra8 for the East/Central/South African (ECSA) genotype of CHIKV is restrictive, and the involvement of other cryptic factors for their infection is being considered.

After binding to target cells, CHIKV is internalized via receptor-mediated endocytosis and the subsequent membrane fusion in acidic endosomes (Bernard et al., 2010; Kielian et al., 2010; Sourisseau et al., 2007). Vancini et al. showed that (1) an alphavirus infection proceeds without endocytosis, (2) the membrane fusion occurs at the plasma membrane, and (3) Sindbis virus (the prototype of the genus *Alphavirus*) associated with the cell plasma membrane forms a pore structure to directly deliver its genomic RNA into the cytoplasm (Vancini et al., 2013). Thus, there is some controversy regarding the early phase of the viral life cycle, and the details of how to change the viral particle structure in the entry steps are unclear.

Here we report the successful production of CHIK virus-like particles (CHIK-VLPs) tagged with enhanced green fluorescent protein (EGFP), i.e., CHIK-VLP-EGFP, by using the ECSA genotype of CHIKV, Ross strain (Robinson, 1955; Ross, 1956) gene (GenBank accession no. AF490259), and we describe the visualization of the attachment of CHIKV to the target cell membrane and the tracing of its fate in subsequent steps. The binding manner of CHIK-VLP-EGFP to the target cell was identical to that of native CHIKV, and most of the EGFP signal promptly disappeared within 30 min in Vero cells. We report the kinetics of CHIK-VLP-EGFP under various conditions including treatment with anti-CHIKV anti-serum, the treatment of target cells affecting the CHIKV membrane fusion at the endosome, and inoculation to some cell lines showing different susceptibilities to CHIKV infections. Our results demonstrate that CHIK-VLP-EGFP will be a useful tool for analyzing the entry phase of CHIKV.

2. Experimental procedures

2.1. Cells and viruses

A baby hamster kidney fibroblast cell line (BHK-21), an African green monkey kidney cell line (Vero), a human astrocytoma cell line (U251MG) (Bigner et al., 1981), and a human alveolar adenocarcinoma cell line (A549) were maintained in Eagle's minimum essential medium (MEM) supplemented with 10% (vol/vol) fetal bovine serum (FBS), 50 units/ml penicillin, and 50 μg/ml streptomycin. A human embryonic kidney cell line (293 T) was maintained in Dulbecco's modified MEM (D-MEM) supplemented with 10% FBS, 50 units/ml penicillin, and 50 μg/ml streptomycin. HAP1 cells (Carette et al., 2009) and the N-sulfated heparan sulfate (HS)-negative HAP1 derivative cell line HAP1ΔNDST1 and its derivative cell lines (HAP1ΔNDST1 transduced with pMX empty vector, HAP1ΔNDST1/pMX and the N-sulfated HS-positive HAP1ΔNDST1/pMX-NDST1) (Tanaka et al., 2017) were grown in Iscove's modified Dulbecco's medium supplemented with 10% FBS, 50 units/ml penicillin, and 50 μg/ml streptomycin. CHIKV Ross strain was inoculated into BHK cells and propagated. The culture supernatant containing CHIKV was clarified by low-speed centrifugation, and aliquots of the supernatant were stored at −80 °C until use.

2.2. Plasmids, antibodies, and reagents

Native CHIKV was recovered from the culture supernatants of the infected BHK cells, and we extracted the viral genomic RNA using a QIAamp Viral RNA Mini kit (Qiagen, Hilden, Germany). First-strand cDNA was synthesized using a Sensiscript reverse transcription kit (Qiagen) with a poly(dT)20 + NotI + XbaI primer. We amplified the whole structural protein (capsid and envelope protein, C-E3-E2-6k-E1) gene of CHIKV Ross strain using a sense primer containing an artificial SacI site (SacI-CHIKV-C-For: 5′-AAAGAGCTCATGGAGTTCATCCCA ACC-3′) and an antisense primer containing an artificial NheI site (NheI-CHIKV-E1-Rev: 5′-TTTGCTAGCTTAGTGCCTGCTGAACGA-3′).

We cloned the polymerase chain reaction (PCR) product into the mammalian expression plasmid pCAGGS, and we designated the construct as pCAGGS/CHIKV-CE. We amplified the envelope protein gene (CHIKV- E3-E2-6k-E1) by using a sense primer containing a SacI site and an in-frame artificial initiation codon (SacI-ATG- CHIKV-E3-For: AAAGAGCTCATGAGTCTTGCCATC) and the antisense primer, NheI-CHIKV-E1-Rev, and cloned it into pCAGGS. The construct was designated as pCAGGS/CHIKV-E.

The EGFP gene was ligated with the flexible linker, G4S tandem repeats, $(Gly\text{-}Gly\text{-}Gly\text{-}Gly\text{-}Ser)_4$-Ala-Arg-$(Gly\text{-}Gly\text{-}Gly\text{-}Gly\text{-}Ser)_4$, to generate the G4S-EGFP. The G4S-EGFP gene was inserted into the 3′ terminal region of E1 of the plasmid, pCAGGS/CHIKV-CE, and pCAGGS/CHIKV-E. We designated these constructs as pCAGGS/CHIKV-CE-EGFP and pCAGGS/CHIKV-E-EGFP and used them to produce the fusion proteins CHIKV-CE-EGFP and CHIKV-E-EGFP.

For the detection of viral antigens, we used anti-CHIKV rabbit serum and anti-CHIKV-E2 mouse monoclonal antibodies (mAb clones CHE24 and CHE29) which were developed in our lab, and anti-CHIKV-E1 mouse mAb clone 6A11 (EMD Millipore, Billerica, MA, USA) and clone CHE22, which was developed in our lab. As the detector antibodies, we used anti-GFP rabbit IgG polyclonal antibody (Invitrogen, Carlsbad, CA), anti-beta-actin monoclonal antibody (Sigma-Aldrich, St. Louis, MO), horseradish peroxidase (HRP)-conjugated goat anti-rabbit Ig (Dako, Glostrup, Denmark), HRP-conjugated goat anti-mouse Ig (Dako), Alexa Fluor 594-coupled anti-mouse IgG (H + L), Alexa Fluor 594-anti-rabbit IgG (H + L) (Invitrogen), and 15-nm colloidal gold particle-conjugated goat anti-rabbit IgG (BBI Solutions, Cardiff, UK). Bafilomycin A1was purchased from Abcam (Cambridge, UK) and used at a concentration of 200 nM in the culture medium.

2.3. The preparation of the replication-deficient VSV vectors

We prepared a replication-deficient recombinant vesicular stomatitis virus (VSV) capable of expressing luciferase, i.e., VSVΔG-luci (VSVG), as described (Tani et al., 2010). Replication-deficient luciferase-expressing VSVs pseudotyped with CHIKV-E-EGFP were prepared as follows. The 293 T cells were grown to 50%–70% confluence on collagen-coated tissue culture plates and then transfected with pCAGGS/CHIKV-E-EGFP or pCAGGS empty vector. After 24 h of incubation, the cells were inoculated with VSVΔG-luci(VSVG) at a multiplicity of infection (MOI) of 1–2. After 2–3 h of incubation for viral adsorption, the cells were extensively washed with fresh medium, and then D-MEM supplemented with 2% FBS and 10 mM HEPES (pH 7.0) was added.

The culture supernatants containing pseudotype VSVΔG-luci (CHIKV-E-EGFP) or VSVΔG-luci(−) were harvested after 18–24 h of incubation at 37 °C. The culture supernatant was clarified by low-speed centrifugation, and aliquots of the supernatant containing these pseudotype viruses were stored at −80 °C until use. The infectivity of the virus was determined by measuring the luciferase activities with a Steady-Glo luciferase assay system (Promega, Madison, WI) according to the manufacturer's protocol.

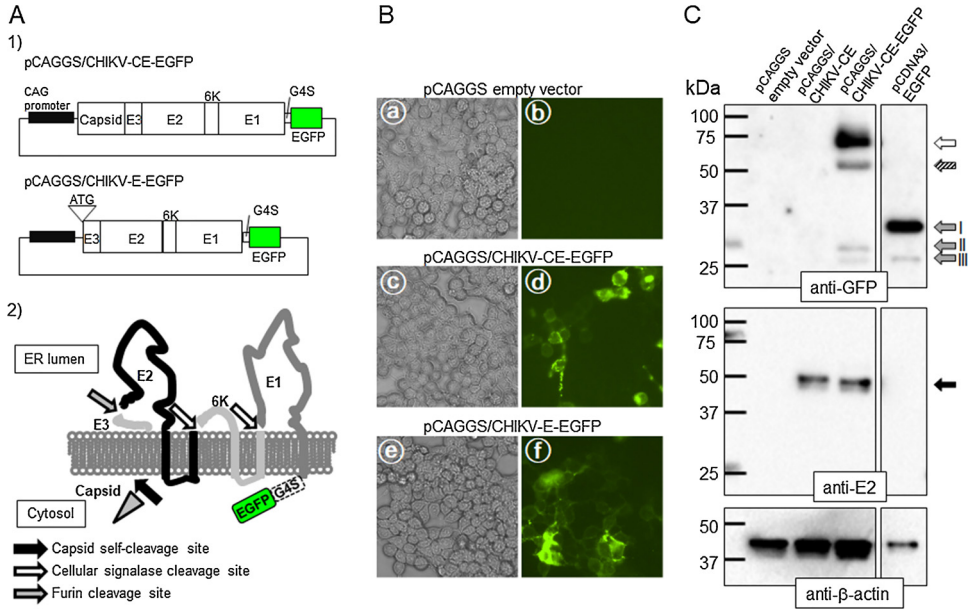

Fig. 1. Schematic representation of the plasmids and the deduced configuration of recombinant structural proteins and their expression. A: (1) The construction of pCAGGS/CHIKV-CE-EGFP and pCAGGS/CHIKV-E-EGFP is shown. (2) A possible configuration of the structural proteins on the endoplasmic reticulum (ER) membrane of the cells transfected with pCAGGS/CHIKV-CE-EGFP. B: 293 T cells transfected with pCAGGS empty vector (a,b), pCAGGS/CHIKV-CE-EGFP (c,d), or pCAGGS/CHIKV-E-EGFP (e,f) were observed under a fluorescence microscope using a 20X objective (b,d,f). C: Western blot analysis of the CHIKV structural protein fused with the EGFP. Cell lysates of 293 T cells transfected with pCAGGS empty vector, pCAGGS/CHIKV-CE, pCAGGS/CHIKV-CE-EGFP, or pCDNA3-EGFP were separated by SDS-PAGE. E1 proteins fused with EGFP (*white arrow*) and its cleavage form (*shuttered arrow*), approx. 27-kDa EGFP (*gray arrow* I) and its cleavage form (approx. 25–26 kDa; *gray arrows* II and III) were detected with the anti-GFP rabbit IgG. CHIKV-E2 antigen (approx. 50 kDa; *black arrow*) was detected with the anti-CHIKV-E2 mouse mAb clone CHE29. As a loading control, beta-actin was detected.

2.4. Western blotting

For the evaluation of the expressions of CHIKV-CE-EGFP and CHIKV-E-EGFP, cell lysates containing the viral antigens were separated by sodium dodecyl sulfate-polyacrylamide gel electrophoresis (SDS-PAGE) and blotted onto a polyvinylidene fluoride (PVDF) membrane. The membrane was treated overnight at 4 °C with a blocking buffer (5% skim milk in phosphate-buffered saline [PBS] containing 0.1% Tween-20 [PBST]) and then incubated for 2 h at room temperature (RT) or overnight at 4 °C with anti-CHIKV rabbit serum (1:500–1000 in blocking buffer), anti-CHIKV-E1 monoclonal antibody, clone 6A11 (EMD Millipore), and clone CHE22 (1:100 in blocking buffer) or anti-GFP rabbit IgG polyclonal antibody (Invitrogen) (1:500–1000 dilution in blocking buffer).

The membranes were then washed with PBST 4–5 times and incubated for 1 h at RT with HRP-conjugated goat anti-rabbit Ig or HRP-conjugated goat anti-mouse Ig (Dako) (1:10,000–15,000 in blocking buffer). After 4–5 washes with PBST, the protein bands were detected with a Western Lightning ECL Pro substrate (PerkinElmer Life Sciences, Boston, MA).

2.5. The production and purification of GFP-tagged CHIK-VLP

For the production and purification of GFP-tagged CHIK-VLPs, CHIK-VLP-EGFP and 293 T cells were plated into six tissue culture dishes (7×10^6 cells/150-mm-dia. dish) at 1 day before transfection, and the cells were transfected with pCAGGS/CHIKV-CE-EGFP (8 μg/dish) using X-*tremeGENE9* DNA *Transfection Reagent* (Roche Diagnostics, Mannheim, Germany).

The cells were incubated at 37 °C for 4 days and then split into ten 150-mm-dia. dishes, and the CHIK-VLP-EGFPs released into the culture supernatant were collected at 2, 3, and 4 days post-transfection (dpt). A total of 600 ml of the culture supernatant was centrifuged at 1,000*g* for 5 min to remove the cell debris and further clarified by centrifugation at 10,000*g* for 20 min at 4 °C in an SW32 Ti rotor (Beckman Coulter, Brea, CA). The CHIK-VLP-EGFPs were concentrated by ultracentrifugation through a 15% sucrose cushion at 100,000*g* for 2 h at 4 °C.

The pellet was gently resuspended in TNE buffer and then layered onto a 15%–45% (w/w) continuous sucrose gradient and centrifuged at 100,000*g* for 2 h at 4 °C in the SW32 Ti rotor. Twenty fractions were collected, and the sucrose density was measured. The fractions containing CHIK-VLP-EGFPs were determined by a western blot analysis, then pooled, diluted in TNE buffer and centrifuged at 100,000*g* for 2 h at 4 °C. The concentration of the purified CHIK-VLP-EGFPs was determined by the Bradford method as outlined by the manufacturer (Bio-Rad).

2.6. Immunoelectron microscopy (IEM)

We used the purified CHIK-VLP-EGFPs to coat a copper grid for 10 min at RT. The grid was blocked with PBS containing 1% bovine serum albumin for 15 min at RT and then incubated with anti-CHIKV rabbit serum at a dilution of 1:100 for 2 h at RT. After six washes with PBS, 15 nm gold-labeled anti-rabbit IgG(H + L) goat antibody (BBI Solutions) at a dilution of 1:100 was added and incubated for 1 h at RT. After six washes with PBS, the sample was stained with uranyl acetate and examined under a transmission electron microscope (TEM) (model JEM-1010; JEOL, Tokyo) working at 80 kV.

2.7. Detection of CHIK-VLP-EGFP signals in target cells

Purified CHIK-VLP-EGFP was inoculated into target cells in two dishes, followed by 1-hr incubation at 4 °C, and then the dishes were washed once with fresh medium. One dish was then fixed by PBS containing 4% paraformaldehyde (4% PFA in PBS), and the other dish was then incubated at 37 °C for 30 min and fixed. Cell-bound CHIK-VLP-EGFPs were detected by a confocal fluorescent microscope as the EGFP puncta.

2.8. Fluorescence microscopy and laser scanning confocal microscopy

To detect the CHIK-VLP-EGFPs in the cells, we acquired EGFP signals with a Nikon eclipse Ti fluorescence microscope or a Nikon C2+ laser scanning confocal microscope. The obtained images were processed by NIS-elements software and Adobe Photoshop software. The number or the area of CHIK-VLP-EGFP particles on target cells was measured by using the 'Analyze Particles' command of ImageJ software.

3. Results

3.1. The structure of the envelope protein tagged with the EGFP expressed in the transfected cells

We introduced EGFP into the C-terminal of cytoplasmic domain of the viral envelope protein (Fig. 1A). To examine the properties of the EGFP-tagged CHIKV structural proteins, we transfected 293 T cells with two expression plasmids: pCAGGS/CHIKV-CE-EGFP and pCAGGS/CHIKV-E-EGFP. The cells transfected with these expression vectors showed stable substantial green fluorescence (Fig. 1B). The cells were collected and examined by SDS-PAGE and western blotting using anti-CHIKV E2 antibody and anti-GFP antibody. As can be seen in Fig. 1C, the cells transfected with pCAGGS/CHIKV-CE or pCAGGS/CHIKV-CE-EGFP expressed E2 protein with a predicted molecular mass of ˜50 kDa. The E1 protein fused with EGFP, i.e., E1-EGFP, had a predicted molecular mass of ˜78 kDa. We observed the cleavage form of E1-EGFP (< 60 kDa) and the cleavage form of EGFP (whose size is < 27 kDa of authentic EGFP) in these cell lysates.

3.2. The properties of CHIKV-E protein tagged with the EGFP expressed in the VSV-CHIKV pseudotype particle

To examine the biological properties of E-EGFP in the viral particle, we constructed the VSV pseudotype virus bearing CHIKV-E-EGFP in its envelope and then examined its infectivity. VSVΔG-luci(CHIKV-E-EGFP) showed high infectivity to HAP1 wild-type cells but low infectivity to the N-sulfated heparan sulfate-negative HAP1 mutant, HAP1ΔNDSTl, and this pseudotype virus infectivity was neutralized by anti-CHIKV rabbit serum (Fig. 2). These results are the same as those of a study that used the VSVΔG-luci(CHIKV-E) pseudotype (Tanaka et al., 2017), and they indicated that the CHIKV-E protein fused with EGFP at the 3′ terminal end of E1 (i.e., E1-EGFP) works sufficiently for VSVΔG-luci(CHIKV-E-EGFP) pseudotype virus infection at the viral entry steps. We thus infer that CHIKV-E-EGFP can mediate the viral internalization consisting of the binding, endocytosis, and membrane fusion in the early endosome.

3.3. The production and characterization of CHIKV-like particles (CHIK-VLPs) tagged with EGFP (CHIK-VLP-EGFP)

To confirm the formation of CHIKV-like particles (CHIK-VLPs) bearing EGFP (CHIK-VLP-EGFP), we harvested the culture supernatants of 293 T cells transfected with pCAGGS/CHIKV-CE-EGFP at 2, 3, and 4 dpt and fractionated the supernatants by sucrose gradient ultracentrifugation. The results demonstrated that the fractions mainly from 20%–30% sucrose densities were positive for the approx. 50-kDa CHIKV-E antigen detected by rabbit anti-CHIKV serum and the approx. 75-kDa CHIKV-E1-EGFP antigen detected by anti-GFP rabbit IgG (Fig. 3). These fractions contained a few EGFP antigens whose size corresponded to the authentic EGFP (approx. 27 kDa), suggesting that some EGFP fragments were present inside the CHIK-VLP-EGFP particle (Fig. 3B).

To confirm whether spherical particles with the CHIKV antigen exist in these CHIKV antigen-positive fractions, we incubated copper grids that had absorbed the purified CHIKV antigen-positive fractions with a primary antibody, anti-CHIKV rabbit serum, followed by 15-nm colloidal gold particles conjugated with goat anti-rabbit IgG. We were able to detect the spherical particles with external dias. of 50–70 nm labeled by gold particles (Fig. 3C). These gold-labeled particles were not observed when the normal rabbit serum was used as the primary antibody. The sizes of CHIKV and CHIK-VLP were reported to be 50–60 nm in dia. (Noranate et al., 2014), and our CHIK-VLP-EGFP also has the same size as normal CHIK-VLPs. These results indicated that the CHIK-VLP-EGFPs were successfully formed.

To test whether the purified CHIK-VLP-EGFPs could be detected as EGFP dots when they were inoculated to the target cells, we observed Vero cells inoculated with purified CHIK-VLP-EGFPs under a confocal microscope. Punctate EGFP signals were observed on the cells which were inoculated with purified CHIK-VLP-EGFP (Fig. 5A). These EGFP puncta were co-localized with the signal of the CHIKV-E2 antigen detected by anti-CHIKV E2 monoclonal antibody (Fig. 4A,B). The estimated Pearson's correlation coefficient is 0.85.

Since the N-sulfated region of heparan sulfate was recently proposed as a minimum structure that is essential for efficient CHIKV binding and infection (Tanaka et al., 2017), we examined whether the CHIK-VLP-EGFP particles showed the same property as the native CHIKV particles. The CHIK-VLP-EGFPs efficiently bound N-sulfated HS-positive HAP1 wild-type cells but not N-sulfated HS-negative HAP1ΔNDST1 cells (Fig. 4C,D). These results indicate that the CHIK-VLP-EGFPs have the same binding properties to the cell-surface HS as native CHIKV.

3.4. The dynamics of CHIK-VLP-EGFP on target cells

The area of CHIK-VLP-EGFP puncta were significantly decreased to ˜30% of those of the non-treated CHIK-VLP-EGFPs after pretreatment with anti-CHIKV rabbit serum (Fig. 5A). It was reported that the cell surface-bound CHIKV particles translocated via endocytosis to late endosomes and lysosomes within a 15-min incubation in mosquito C6/36 cells (Lee et al., 2013). To examine the dynamics and fate of CHIK-VLP-

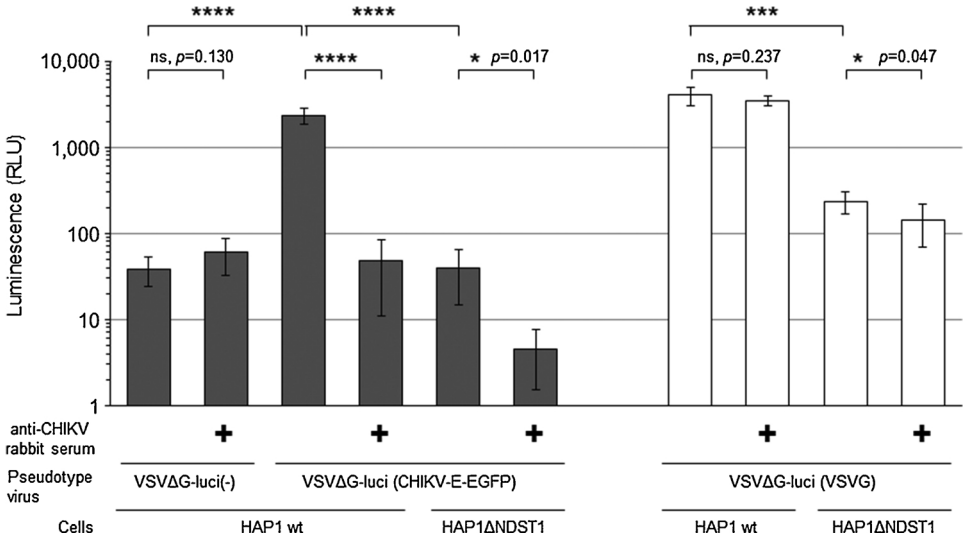

Fig. 2. The infectivity of pseudotype virus bearing CHIKV-E3-1-EGFP.
Wild-type HAP1 and N-sulfated HS-defective HAP1ΔNDST1 cells inoculated with luciferase-expressing the recombinant VSV pseudotype bearing CHIKV-E-EGFP, VSVΔG-luci(CHIKV-E-EGFP), with or without anti-CHIKV rabbit serum at a dilution of 1:50 treatment at 37 °C for 30 min were incubated for 20–24 h, and then the relative light unit (RLU) value of luciferase activity was determined. The pseudotype bearing no envelope protein, VSVΔG-luci (-), and the pseudotype bearing the VSVG protein, VSVΔG-luci(VSVG), were used as the negative control and the internal control, respectively. Data are the mean ± SD of three independent experiments and were evaluated by an unpaired two-tailed t-test. *p < 0.05, ***p < 0.001, ****p < 0.0001.

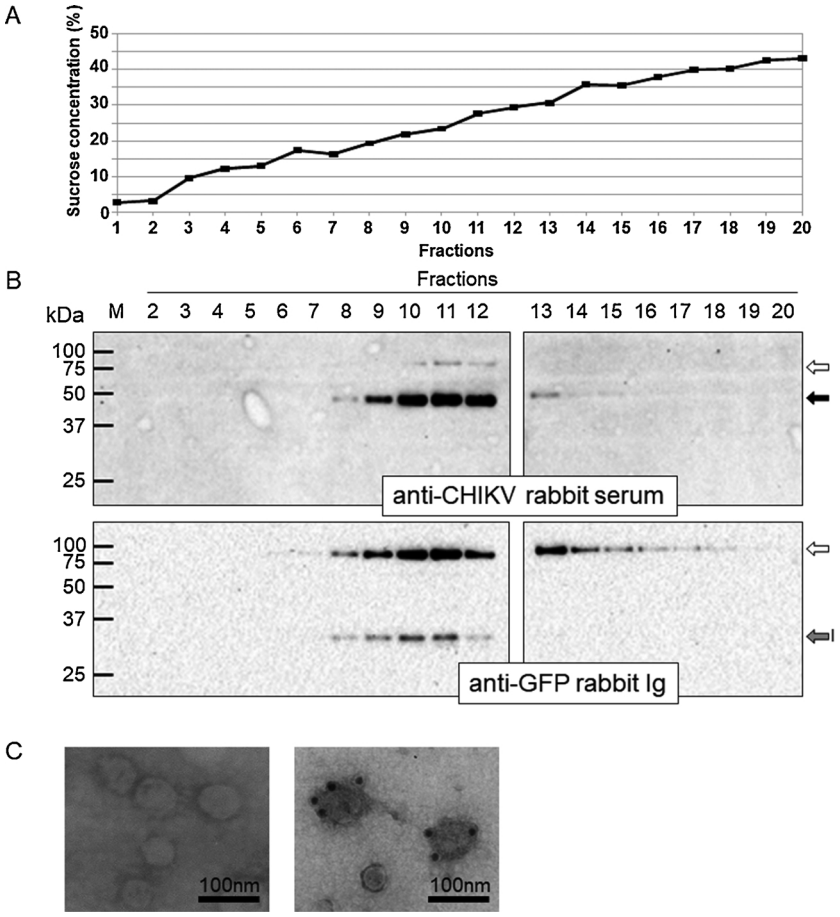

Fig. 3. The purification of CHIK-VLP-EGFP by sucrose gradient ultracentrifugation. A: The sucrose gradient was separated into 20 fractions, and the sucrose concentration of each fraction was measured by a refractometer. B: Each aliquot of the fractions was examined by western blotting using anti-CHIKV rabbit serum (*upper*) or anti-GFP rabbit IgG (*bottom*). CHIKV E1-EGFP (approx. 75 kDa; *white arrow*), CHIKV E2 antigen (approx. 50 kDa; *black arrow*), and the proteins containing an EGFP antigen (approx. 27 kDa; *gray arrow* I) were detected. C: The detection of the formation of CHIK-VLP-EGFPs by electron microscopy. Immunoelectron micrographs of CHIKV antigen reacted with anti-CHIKV-rabbit serum (right panel) or with normal rabbit serum (left panel) and the subsequent reaction with 15-nm gold particle-labeled goat anti-rabbit IgG are shown. Gold particles were detected on the CHIK-VLP-EGFP particles (approx. 50–70 nm dia.). Magnification ×30,000. Scale bar: 100 nm.

EGFPs bound to the target cells, we compared the changes of EGFP puncta detected after the 30 min incubation at 37 °C following the binding by 1 h incubation at 4 °C. We observed that > 80% of these CHIK-VLP-EGFP's puncta in inoculated cells disappeared after incubation at 37 °C for 30 min (Fig. 5A,C,D), but most of the puncta of anti-CHIKV neutralizing rabbit serum-treated CHIK-VLP-EGFP were not decreased (Fig. 5A).

We also frequently observed the aggregated form of CHIK-VLP-EGFP with anti-CHIKV rabbit IgG on the surface of the cells inoculated with anti-CHIKV rabbit serum-treated CHIK-VLP-EGFPs (Fig. 5B). This undiminished EGFP signal of CHIK-VLP-EGFPs seems to be compatible with CHIKV infections that were inhibited by anti-CHIKV neutralizing rabbit serum. Thus, the internalization of CHIK-VLP-EGFP and its subsequent disassembly was inhibited with the use of anti-CHIKV neutralizing rabbit serum.

We next examined whether the reduction of EGFP signals of CHIK-VLP-EGFPs was inhibited by the treatment of the target cells with bafilomycin A1, which is a specific inhibitor of V-ATPase (Bowman et al., 1988; Umata et al., 1990; Yoshimori et al., 1991) and an inhibitor of CHIKV infection (Khan et al., 2010; Kishishita et al., 2013; Nuckols et al., 2014; Sourisseau et al., 2007). We also observed that the reduction of the EGFP signal of CHIK-VLP-EGFPs was inhibited by the treatment of the target cells with bafilomycin A1 (Fig. 5C,D), suggesting that the disassembly of internalized CHIK-VLP-GFP by membrane fusion or lysosomal degradation (or low pH quenching in the lysosome) was inhibited by bafilomycin A1. In these bindings of CHIK-VLP-EGFPs, E1-EGFPs were still observed after the subsequent 30 min incubation at 37 °C under the conditions with or without bafilomycin A1, but their sizes slightly decreased, suggesting that the conformational change or processing of E1-EGFP could be induced.

The original sizes of EGFP (27 kDa; gray arrow I in Fig. 5E) and cleaved EGFP antigens (approx. 26 kDa; gray arrow II) were detected after the 30 min incubation at 37 °C, but rarely detected in the cells treated with bafilomycin A1. These results indicated that the cleaved EGFPs were generated by endosomal or lysosomal acidification, and they also indicated that the elimination of the fluorescence signal of E1-EGFP after the subsequent 30 min incubation at 37 °C is not due to the release of E1-EGFP from the cell surface.

We also attempted to observe the dynamics of native CHIKV by using the anti-CHIKV-E1 mouse mAb, and we observed that the native CHIKV that had been detected as the fluorescent puncta disappeared after the subsequent 30 min incubation at 37 °C; this result is similar to that of CHIK-VLP-EGFPs (Suppl. Fig. S1A,B). The western blotting using anti-CHIKV-E1 monoclonal antibody (clone 6A11) showed that E1 proteins still remained after the incubation at 37 °C (Suppl. Fig. S1C), whereas reducing E1 proteins were detected when the anti-CHIKV-E1 monoclonal antibody (clone CHE22) was used (Suppl. Fig. S1D). These findings indicated that the E1 proteins of cell-bound CHIKV virions changed their conformation and were disassembled and defused during the incubation at 37 °C, and the fluorescence signals were then not detected as the puncta. In contrast, the E2 protein of cell-bound CHIK-VLP-EGFPs after the subsequent 30 min incubation at 37 °C was not detected by the anti-CHIKV-E2 mouse mAb (Fig. 5E) or anti-CHIKV rabbit serum (data not shown) regardless of bafilomycin A1 treatment, suggesting that E2 protein was lost regardless of the endosome pH. These phenomena of the loss of E2 protein were also observed in native CHIKV (Suppl. Fig. S1C). Together these findings led us to propose the model shown in Fig. 6.

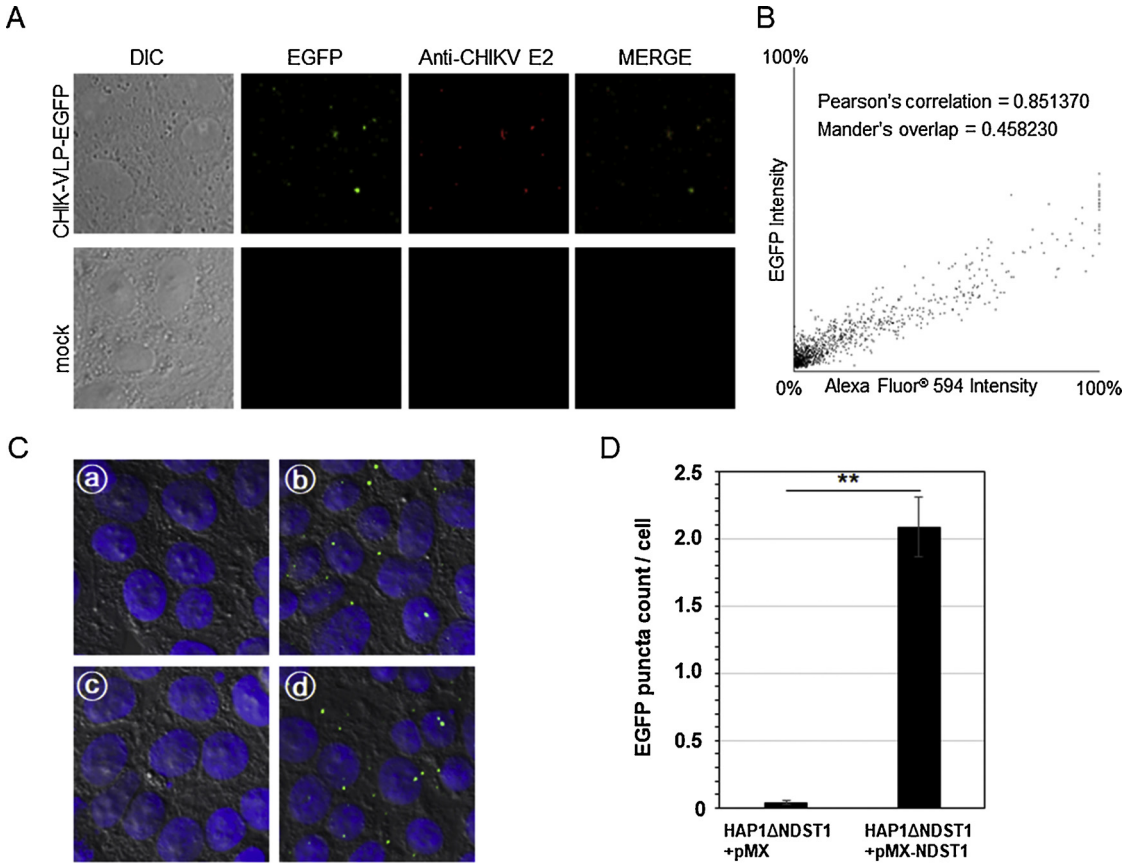

Fig. 4. The detection of CHIK-VLP-EGFP signals in target cells. A: CHIK-VLP-EGFP was inoculated into Vero cells and incubated for 1 h at 4 °C. CHIKV-E antigen was detected by using anti-CHIKV E2 mouse mAb clone CHE24 and anti-mouse IgG (Alexa Fluor® 594 Conjugate). Images were taken using a confocal microscope with a 40 x objective lens. B: Colocalization analysis of EGFP and CHIKV-E2 antigen using NIS-elements software. Scatter plots of EGFP intensity and Alexa Fluor® 594 intensity are shown. Pearson's correlation and Mander's overlap were analyzed. C: The binding activity of CHIK-VLP-EGFP affected the cell-surface HS. Purified CHIK-VLP-EGFP was inoculated into parental HAP1wt (*b*), N-sulfated HS-deficient HAP1/ΔNDST1/pMXpuro cells (*c*) and its rescued cells, i.e., HAP1/ΔNDST1/pMXpuro-NDST1 cells (*d*). No EGFP puncta were observed in the un-inoculated control cells (*a*). Images were taken using a confocal microscope with a 40 x objective lens. D: CHIK-VLP-EGFP exhibited a significant level of binding to N-sulfated HS-expressing cells but not to cells lacking N-sulfated HS expression. Data are the mean ± SD of four confocal fields of one of two independent experiments showing similar results and were evaluated by an unpaired two-tailed t-test. **$p < 0.01$.

3.5. The different elimination rates of CHIK-VLP-EGFP among the cell lines showing different susceptibility

Sourisseau et al. (2007) reported that CHIKV showed binding and infectivity in most adherent but not non-adherent cell lines. They observed that one of the adherent cell lines, i.e., the human alveolar adenocarcinoma cell line A549, was resistant to CHIKV infection. We also observed that A549 cells showed significant resistance to the CHIKV Ross strain, and the ratios of virus-induced cell death were 1/500,000 and 1/8,000 of those of the adherent lines of Vero cells and U251MG cells, respectively (Suppl. Fig. S1A,B). No significant difference in the susceptibility to the CHIKV pseudotype infection was observed between the highly susceptible cell lines (Vero and U251MG) and the poorly susceptible A549 cells (Suppl. Fig. S1C) or in the CHIKV production rate after CHIKV RNA transfection (Suppl. Fig. S1D).

We next examined the kinetics of CHIK-VLP-EGFP in these cell lines. The CHIK-VLP-EGFP bound to the A549 cells, as it had to Vero cells. Although the EGFP signal was promptly eliminated in the highly susceptible Vero and U251MG cells in the 30 min incubation at 37 °C, almost all of the EGFP signal was still observed in A549 cells (Fig. 7A,B), indicating that in A549 cells the elimination of E1-EGFP did not occur and the disassembly of CHIK-VLP-EGFP did not proceed. These findings suggested that the low infectivity of native CHIKV in A549 cells is ascribable to native CHIKV particles' deficit of internalization efficiency.

4. Discussion

Many research groups have examined the dynamic processes of virus infection by using fluorescence-labeled viral particles or virus-like particles. For single particle tracking, GFP fusion protein-labeled viruses were reported to have relatively large sizes which provided additional structural space for the occupation of a sufficient number of GFP molecules to detect a single particle, such as herpes virus (Desai and Person, 1998; Elliott and O'Hare, 1999), African swine fever virus (Hernaez et al., 2006), human immunodeficiency virus (McDonald et al., 2002; Campbell et al., 2007), avian sarcoma and leucosis virus (Padilla-Parra et al., 2012), Pox virus (Ward, 2004), and rabies virus (Klingen et al., 2008). On the other hand, relatively small-size viruses and a virus that has no additional structural space for enough GFP were labeled by a fluorescent dye such as a membrane intercalating dye (e.g., DiD), and amine reactive dye: the adeno-associated viruses (AAVs) (Seisenberger et al., 2001), CHIKV (Hoornweg et al., 2016), dengue virus (van der Schaar et al., 2007, 2008; Ayala-Nunez et al., 2011), virus-like particles of murine polyoma virus (Ewers et al., 2005), hepatitis C virus (Coller et al., 2009), and influenza virus (Lakadamyali et al., 2003).

These fluorescent dye labeling methods are powerful tools for detecting single viral particles, but their use does not always ensure the labeling of most of the viruses, and their labeling has varied considerably between different viral preparations. To simply and quantitatively observe the binding of CHIKV to the cell surface, we herein

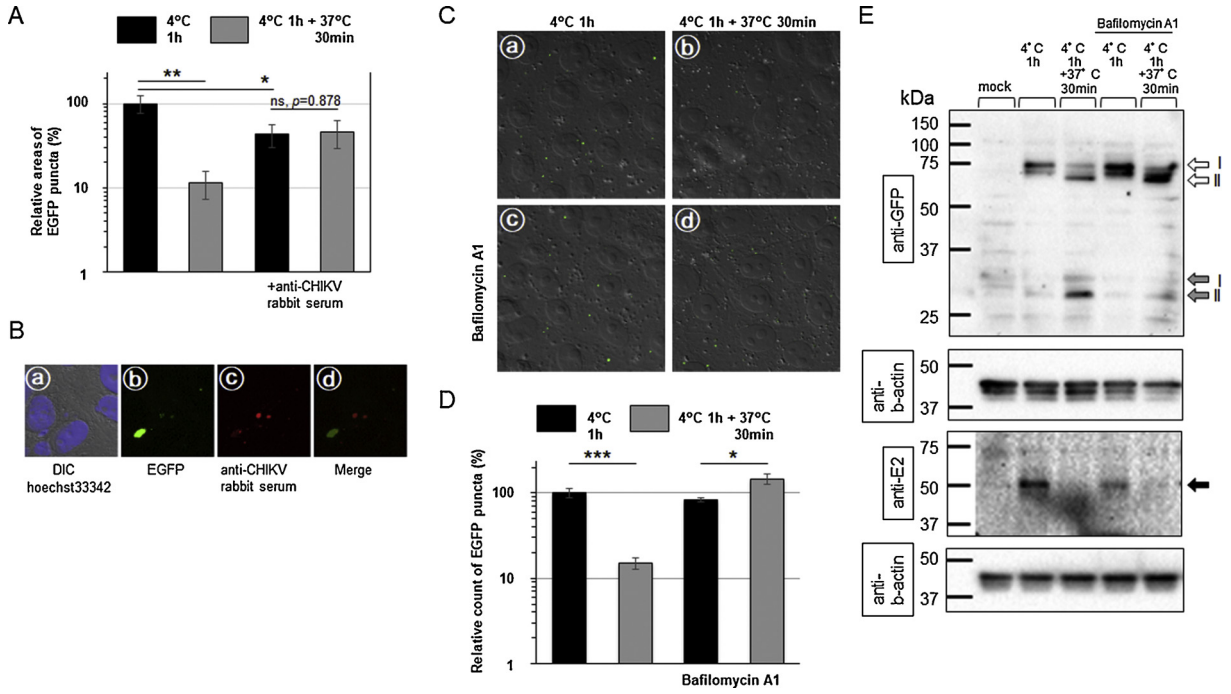

Fig. 5. The reduction of CHIK-VLP-EGFP signals in target cells. A: The effect of anti-CHIKV serum on the kinetics of CHIK-VLP-EGFP. CHIK-VLP-EGFPs treated with or without anti-CHIKV rabbit serum at a dilution of 1:100 were inoculated into Vero cells and the CHIK-VLP-EGFPs were detected by a confocal fluorescent microscope as the EGFP puncta. B: The aggregation of CHIK-VLP-EGFPs. Vero cells inoculated with CHIK-VLP-EGFPs which were treated with anti-CHIKV rabbit serum were incubated at 4 °C for 1 h and then at 37 °C for 30 min. The nuclei of target cells were stained with Hoechst33342 (*a*; DIC field merged with Hoechst33342 staining). EGFP detection (*b*); anti-CHIKV IgGs detected by Alexa Fluor 594-coupled anti-rabbit IgG (H + L) (*c*); and EGFP puncta merged with anti-CHIKV rabbit IgGs detected by Alexa Fluor 594-coupled anti-rabbit IgG (H + L) (*d*). C: CHIK-VLP-EGFP was inoculated into Vero cells in culture with (c,d) or without (a,b) bafilomycin A1 (200 nM). Cells were fixed after 1 h incubation at 4 °C (a,c) or after the 30-min incubation at 37 °C following the 4 °C incubation for 1 h (b,d). Images were taken using a confocal microscope with a 60 x oil immersion objective lens (B and C). D: Bafilomycin A1 treatment inhibited the reduction of EGFP puncta. Data are the mean ± SEM (n = 7–8) of two independent experiments. Significance was evaluated by an unpaired two-tailed t-test. ns: not significant, *p < 0.05, **p < 0.01, ***p < 0.001. E: The western blot analysis of bound CHIK-VLP-EGFP in the target cells treated with or without bafilomycin A1. Vero cell lysates were separated by SDS-PAGE with non-reducing conditions. Blots were probed with anti-GFP rabbit IgG polyclonal antibody and anti-CHIKV-E2 mouse mAb clone CHE29 as indicated. As a loading control, the anti-beta-actin monoclonal antibody was used for detection. Two forms of EGFP-fused E1 antigen: approx. 75 kDa E1-EGFP (*white arrow* I), and < 75 kDa of conformation changed E1-EGFP (*white arrow* II), and two forms releasing EGFP antigens (27 kDa; gray arrow I and approx. 26 kDa of cleaved EGFP; *gray arrow* II), and the approx. 50 kDa E2 antigen (*black arrow*) were detected.

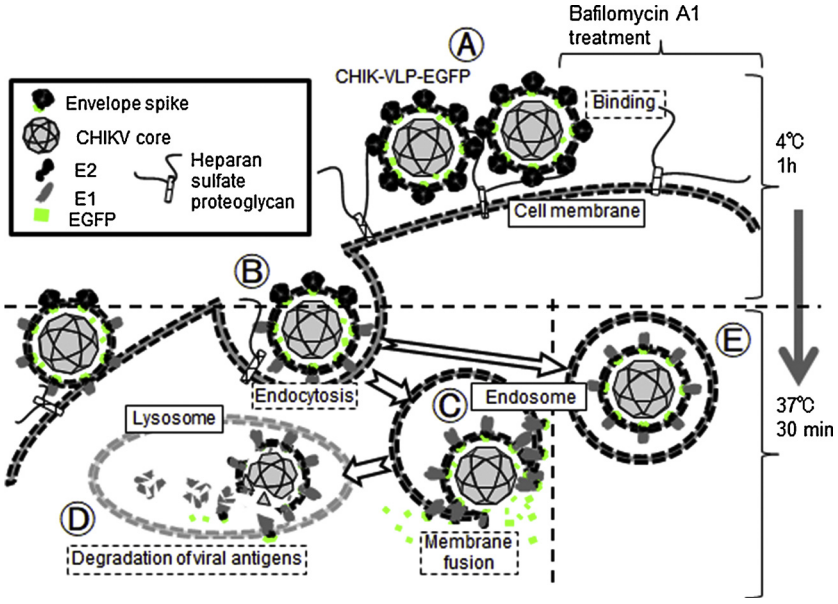

Fig. 6. Overview of the entry step of CHIK-VLP-EGFP, which was deduced by the detection of EGFP signals and by western blotting results. EGFP puncta of CHIK-VLP-EGFPs were detected after the binding step at 4 °C for 1 h (A) and were lost during the subsequent incubation at 37 °C for 30 min (C, D). E2 proteins were lost and E1-EGFP changed its conformation at 37 °C for 30 min (B, C, D and E). E1-EGFP was cleaved at the endosome or lysosome (C, D), and the cleaved EGFPs were defused into the cytoplasm by membrane fusion (C). E1-EGFs was not cleaved and EGFP signals were stable under the condition with bafilomycin A1 treatment (E).

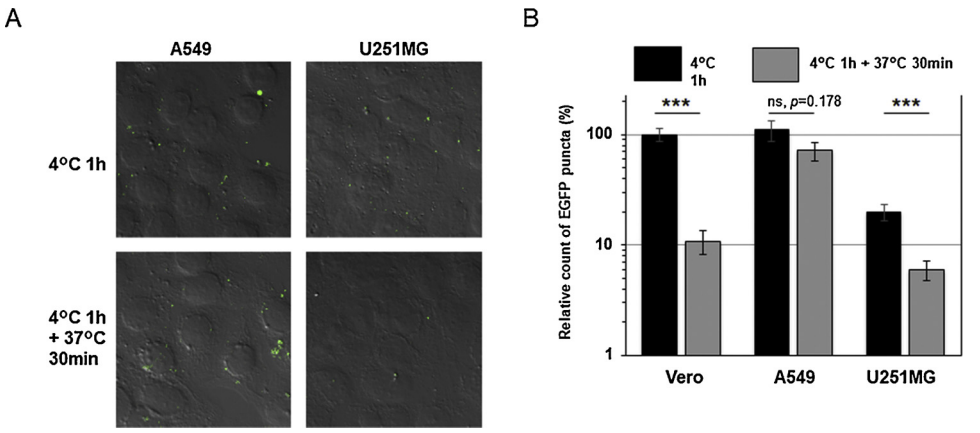

Fig. 7. The differences in the EGFP signal reduction ratio among the cell lines. A: Different bindings of CHIK-VLP-EGFPs in the A549 and U251MG cell lines. Images were taken using a confocal microscope with a 60 x oil immersion objective lens. B: The relative count of EGFP puncta is shown as the percentage of the number of EGFP puncta observed in Vero cells, A549 cells, and U251MG cells at the binding and elimination phases. Data are the mean ± SEM of three independent experiments. Significance was evaluated by an unpaired two-tailed t-test. ns: not significant, ***$p < 0.001$.

created CHIK-VLP-GFP, which is virus-like particles containing fluorescent protein inside the viral envelope. The particle size of alphaviruses such as CHIKV is 60–70 nm in dia. (which is smaller than those of Herpes virus and HIV), and the viral surface is covered with virus membrane proteins in an orderly formation with T = 4 icosahedral symmetry that is composed of a total of 240 E1-E2 heterodimers. Regarding these alphaviruses, there is no report that other proteins can be retained on membrane proteins or can be produced (unlike retroviral particles such as HIV).

The cytoplasmic region of the E2 protein is in contact with the capsid (Jose et al., 2012; Lee et al., 1996; Owen and Kuhn, 1997; Skoging et al., 1996), and it appears that there is not much space between the envelope and the capsid. EGFP fused to the E1 protein via the flexible linker allow the EGFP region could have mobility, so that the EGFP region may move to locate in the small space between the viral core and the envelope of the VLP.

It was reported that GFP-labeled HIV particles were detected as fluorescent particles because it was thought that the average, 100–200 Vpr-GFP molecules are incorporated into a single particle (McDonald et al., 2002). We therefore considered the possibility that the 240-heterodimer consisting of E2 and E1-EGFP protein in a single CHIK-VLP-EGFP particle ensured sufficient fluorescence intensity for the detection of a single particle, and we clearly observed this CHIK-VLP-EGFP in the present study. Since the particle structure of CHIKV-VLP-EGFP is guaranteed to contain the E2 and E1-EGFP proteins and the number of bound particles can be directly measured as the EGFP puncta, our method has an advantage in that it can be evaluated accurately when carrying out viral binding experiments. In addition, our CHIKV-VLP-EGFP can be cryopreserved by the same method as that used for native CHIKV preservation, and it is not infectious material. These are advantages for the reproducibility and safety of the experiments.

Our experiments revealed that the E2 protein was promptly lost during internalization regardless of the endosome pH, and the E1-EGFP protein also changed its conformation during internalization regardless of the endosome pH. These changes were observed in native CHIKV E1 and E2 proteins (Suppl. Fig. S1C,D), suggesting that CHIKV-VLP-EGFP disassembles in a manner that is the same as that used by the native CHIKV. This is an important reason to use CHIKV-VLP-EGFP for the examination of CHIKV internalization. Our results demonstrated that the anti-CHIKV neutralizing serum, the CHIKV internalization-inhibiting reagent, and the susceptibility of some cell lines influence the CHIK-VLP-GFP dynamics. Assessments of the neutralization activity of antibodies, replication-competent GFP-expressing recombinant CHIKV (Tsetsarkin et al., 2006; Deng et al., 2016), luciferase-expressing pseudotyped-lentiviral vector-bearing CHIKV-E protein (Kishishita et al., 2013) and VSV pseudotype virus bearing CHIKV-E (Tanaka et al., 2017) have been developed and are currently in use as effective assays. Analyses using these reporter-gene coding viruses (and pseudo-viruses) which detect the reporter-gene expression after its successful infection are both convenient and highly sensitive. However, these analyses cannot show how the internalization proceeds or how neutralizing antibodies inhibit the CHIKV infection. Our analysis using the CHIK-VLP-EGFP could not assess the binding efficiency at 37 °C because of its disassembly, but it could show the kinetics of inhibition of the viral internalization after binding by its disassembly.

CHIK-VLP-GFP will be useful for examining the inhibiting mechanism of anti-CHIKV antibodies and antiviral compounds that affect the entry phase of CHIKV.

Acknowledgments

We thank Dr. Y. Matsuura (Dept. of Molecular Virology, RIMD) for the recombinant VSVs (VSVΔG*-G and VSVΔG-luci-G) and the pCAGGS/VSVG plasmid. We thank Dr. T. Shioda (Dept. of Viral Infection, RIMD) for critical advice. This work was supported by Japan Society for the Promotion of Science (Grant Number: 16K09934), by Japan Initiative for Global Research Network on Infectious Diseases (J-GRID) (Grant Number: JP18fm0108003), and by Japan Agency for Medical Research and Development (AMED) (Grant Number: JP19fk0108036, JP18fk0108036h0002).

Appendix A. Supplementary data

Supplementary material related to this article can be found, in the online version, at doi:https://doi.org/10.1016/j.virusres.2019.197732.

References

Ashbrook, A.W., Burrack, K.S., Silva, L.A., Montgomery, S.A., Heise, M.T., Morrison, T.E., Dermody, T.S., 2014. Residue 82 of the Chikungunya virus E2 attachment protein modulates viral dissemination and arthritis in mice. J. Virol. 88 (21), 12180–12192. https://doi.org/10.1128/JVI.01672-14.

Ayala-Nunez, N.V., Wilschut, J., Smit, J.M., 2011. Monitoring virus entry into living cells using DiD-labeled dengue virus particles. Methods 55 (2), 137–143. https://doi.org/10.1016/j.ymeth.2011.07.009.

Bernard, E., Solignat, M., Gay, B., Chazal, N., Higgs, S., Devaux, C., Briant, L., 2010. Endocytosis of chikungunya virus into mammalian cells: role of clathrin and early endosomal compartments. PLoS One 5 (7), e11479.

Bigner, D.D., Bigner, S.H., Ponten, J., Westermark, B., Mahaley, M.S., Ruoslahti, E., Herschman, H., Eng, L.F., Wikstrand, C.J., 1981. Heterogeneity of genotypic and phenotypic characteristics of fifteen permanent cell lines derived from human gliomas. J. Neuropathol. Exp. Neurol. 40 (3), 201–229.

Boggs, W.M., Hahn, C.S., Strauss, E.G., Strauss, J.H., Griffin, D.E., 1989. Low pH-dependent Sindbis virus-induced fusion of BHK cells: differences between strains correlate with amino acid changes in the E1 glycoprotein. Virology 169 (2), 485–488.

Bowman, E.J., Siebers, A., Altendorf, K., 1988. Bafilomycins: a class of inhibitors of membrane ATPases from microorganisms, animal cells, and plant cells. Proc. Natl. Acad. Sci. U. S. A. 85 (21), 7972–7976.

Burt, F.J., Rolph, M.S., Rulli, N.E., Mahalingam, S., Heise, M.T., 2012. Chikungunya: a re-emerging virus. Lancet 379 (9816), 662–671.

Campbell, E.M., Perez, O., Melar, M., Hope, T.J., 2007. Labeling HIV-1 virions with two fluorescent proteins allows identification of virions that have productively entered

the target cell. Virology 360 (2), 286–293.
Carette, J.E., Guimaraes, C.P., Varadarajan, M., Park, A.S., Wuethrich, I., Godarova, A., Kotecki, M., Cochran, B.H., Spooner, E., Ploegh, H.L., Brummelkamp, T.R., 2009. Haploid genetic screens in human cells identify host factors used by pathogens. Science 326 (5957), 1231–1235.
Cheng, R.H., Kuhn, R.J., Olson, N.H., Rossmann, M.G., Choi, H.K., Smith, T.J., Baker, T.S., 1995. Nucleocapsid and glycoprotein organization in an enveloped virus. Cell 80 (4), 621–630.
Coller, K.E., Berger, K.L., Heaton, N.S., Cooper, J.D., Yoon, R., Randall, G., 2009. RNA interference and single particle tracking analysis of hepatitis C virus endocytosis. PLoS Pathog. 5 (12), e1000702.
Das, T., Jaffar-Bandjee, M.C., Hoarau, J.J., Krejbich Trotot, P., Denizot, M., Lee-Pat-Yuen, G., Sahoo, R., Guiraud, P., Ramful, D., Robin, S., Alessandri, J.L., Gauzere, B.A., Gasque, P., 2010. Chikungunya fever: CNS infection and pathologies of a re-emerging arbovirus. Prog. Neurobiol. 91 (2), 121–129.
Deng, C.L., Liu, S.Q., Zhou, D.G., Xu, L.L., Li, X.D., Zhang, P.T., Li, P.H., Ye, H.Q., Wei, H.P., Yuan, Z.M., Qin, C.F., Zhang, B., 2016. Development of neutralization assay using an eGFP chikungunya virus. Viruses 8 (7), 181.
Desai, P., Person, S., 1998. Incorporation of the green fluorescent protein into the herpes simplex virus type 1 capsid. J. Virol. 72 (9), 7563–7568.
Economopoulou, A., Dominguez, M., Helynck, B., Sissoko, D., Wichmann, O., Quenel, P., Germonneau, P., Quatresous, I., 2009. Atypical Chikungunya virus infections: clinical manifestations, mortality and risk factors for severe disease during the 2005-2006 outbreak on Reunion. Epidemiol. Infect. 137 (4), 534–541.
Elliott, G., O'Hare, P., 1999. Live-cell analysis of a green fluorescent protein-tagged herpes simplex virus infection. J. Virol. 73 (5), 4110–4119.
Ewers, H., Smith, A.E., Sbalzarini, I.F., Lilie, H., Koumoutsakos, P., Helenius, A., 2005. Single-particle tracking of murine polyoma virus-like particles on live cells and artificial membranes. Proc. Natl. Acad. Sci. U. S. A. 102 (42), 15110–15115.
Hernaez, B., Escribano, J.M., Alonso, C., 2006. Visualization of the African swine fever virus infection in living cells by incorporation into the virus particle of green fluorescent protein-p54 membrane protein chimera. Virology 350 (1), 1–14.
Hoornweg, T.E., van Duijl-Richter, M.K.S., Ayala Nunez, N.V., Albulescu, I.C., van Hemert, M.J., Smit, J.M., 2016. Dynamics of Chikungunya virus cell entry unraveled by single-virus tracking in living cells. J. Virol. 90 (9), 4745–4756.
Jose, J., Przybyla, L., Edwards, T.J., Perera, R., Burgner 2nd, J.W., Kuhn, R.J., 2012. Interactions of the cytoplasmic domain of Sindbis virus E2 with nucleocapsid cores promote alphavirus budding. J. Virol. 86 (5), 2585–2599.
Jose, J., Snyder, J.E., Kuhn, R.J., 2009. A structural and functional perspective of alphavirus replication and assembly. Future Microbiol. 4 (7), 837–856.
Justman, J., Klimjack, M.R., Kielian, M., 1993. Role of spike protein conformational changes in fusion of Semliki Forest virus. J. Virol. 67 (12), 7597–7607.
Khan, M., Santhosh, S.R., Tiwari, M., Lakshmana Rao, P.V., Parida, M., 2010. Assessment of in vitro prophylactic and therapeutic efficacy of chloroquine against Chikungunya virus in vero cells. J. Med. Virol. 82 (5), 817–824.
Kielian, M., Chanel-Vos, C., Liao, M., 2010. Alphavirus entry and membrane fusion. Viruses 2 (4), 796–825.
Kielian, M., Helenius, A., 1985. pH-induced alterations in the fusogenic spike protein of Semliki Forest virus. J. Cell Biol. 101 (6), 2284–2291.
Kishishita, N., Takeda, N., Anuegoonpipat, A., Anantapreecha, S., 2013. Development of a pseudotyped-lentiviral-vector-based neutralization assay for chikungunya virus infection. J. Clin. Microbiol. 51 (5), 1389–1395.
Klingen, Y., Conzelmann, K.K., Finke, S., 2008. Double-labeled rabies virus: live tracking of enveloped virus transport. J. Virol. 82 (1), 237–245.
Lakadamyali, M., Rust, M.J., Babcock, H.P., Zhuang, X., 2003. Visualizing infection of individual influenza viruses. Proc. Natl. Acad. Sci. U. S. A. 100 (16), 9280–9285.
Lee, R.C., Hapuarachchi, H.C., Chen, K.C., Hussain, K.M., Chen, H., Low, S.L., Ng, L.C., Lin, R., Ng, M.M., Chu, J.J., 2013. Mosquito cellular factors and functions in mediating the infectious entry of chikungunya virus. PLoS Negl. Trop. Dis. 7 (2), e2050.
Lee, S., Owen, K.E., Choi, H.K., Lee, H., Lu, G., Wengler, G., Brown, D.T., Rossmann, M.G., Kuhn, R.J., 1996. Identification of a protein binding site on the surface of the alphavirus nucleocapsid and its implication in virus assembly. Structure 4 (5), 531–541.
Leung, J.Y., Ng, M.M., Chu, J.J., 2011. Replication of alphaviruses: a review on the entry process of alphaviruses into cells. Adv. Virol. 2011, 249640.
McDonald, D., Vodicka, M.A., Lucero, G., Svitkina, T.M., Borisy, G.G., Emerman, M., Hope, T.J., 2002. Visualization of the intracellular behavior of HIV in living cells. J. Cell Biol. 159 (3), 441–452.
Morrison, T.E., 2014. Reemergence of chikungunya virus. J. Virol. 88 (20), 11644–11647.
Noranate, N., Takeda, N., Chetanachan, P., Sittisaman, P., A-nuegoonpipat, A., Anantapreecha, S., 2014. Characterization of chikungunya virus-like particles. PLoS One 9 (9), e108169.
Nuckols, J.T., McAuley, A.J., Huang, Y.J., Horne, K.M., Higgs, S., Davey, R.A., Vanlandingham, D.L., 2014. pH-Dependent entry of chikungunya virus fusion into mosquito cells. Virol. J. 11, 215.
Omar, A., Koblet, H., 1988. Semliki Forest virus particles containing only the E1 envelope glycoprotein are infectious and can induce cell-cell fusion. Virology 166 (1), 17–23.
Owen, K.E., Kuhn, R.J., 1997. Alphavirus budding is dependent on the interaction between the nucleocapsid and hydrophobic amino acids on the cytoplasmic domain of the E2 envelope glycoprotein. Virology 230 (2), 187–196.
Padilla-Parra, S., Marin, M., Kondo, N., Melikyan, G.B., 2012. Synchronized retrovirus fusion in cells expressing alternative receptor isoforms releases the viral core into distinct sub-cellular compartments. PLoS Pathog. 8 (5), e1002694.
Parola, P., de Lamballerie, X., Jourdan, J., Rovery, C., Vaillant, V., Minodier, P., Brouqui, P., Flahault, A., Raoult, D., Charrel, R.N., 2006. Novel chikungunya virus variant in travelers returning from Indian Ocean islands. Emerg. Infect. Dis. 12 (10), 1493–1499.
Pialoux, G., Gauzere, B.A., Jaureguiberry, S., Strobel, M., 2007. Chikungunya, an epidemic arbovirosis. Lancet Infect. Dis. 7 (5), 319–327.
Robin, S., Ramful, D., Le Seach, F., Jaffar-Bandjee, M.C., Rigou, G., Alessandri, J.L., 2008. Neurologic manifestations of pediatric chikungunya infection. J. Child Neurol. 23 (9), 1028–1035.
Robinson, M.C., 1955. An epidemic of virus disease in Southern Province, Tanganyika Territory, in 1952-53. I. Clinical features. Trans. R. Soc. Trop. Med. Hyg. 49 (1), 28–32.
Ross, R.W., 1956. The Newala epidemic. III. The virus: isolation, pathogenic properties and relationship to the epidemic. J. Hyg. (Lond.) 54 (2), 177–191.
Rostand, K.S., Esko, J.D., 1997. Microbial adherence to and invasion through proteoglycans. Infect. Immun. 65 (1), 1–8.
Sanz, M.A., Rejas, M.T., Carrasco, L., 2003. Individual expression of sindbis virus glycoproteins. E1 alone promotes cell fusion. Virology 305 (2), 463–472.
Seisenberger, G., Ried, M.U., Endress, T., Buning, H., Hallek, M., Brauchle, C., 2001. Real-time single-molecule imaging of the infection pathway of an adeno-associated virus. Science 294 (5548), 1929–1932.
Silva, L.A., Khomandiak, S., Ashbrook, A.W., Weller, R., Heise, M.T., Morrison, T.E., Dermody, T.S., 2014. A single-amino-acid polymorphism in Chikungunya virus E2 glycoprotein influences glycosaminoglycan utilization. J. Virol. 88 (5), 2385–2397.
Simizu, B., Yamamoto, K., Hashimoto, K., Ogata, T., 1984. Structural proteins of Chikungunya virus. J. Virol. 51 (1), 254–258.
Skoging, U., Vihinen, M., Nilsson, L., Liljestrom, P., 1996. Aromatic interactions define the binding of the alphavirus spike to its nucleocapsid. Structure 4 (5), 519–529.
Smith, T.J., Cheng, R.H., Olson, N.H., Peterson, P., Chase, E., Kuhn, R.J., Baker, T.S., 1995. Putative receptor binding sites on alphaviruses as visualized by cryoelectron microscopy. Proc. Natl. Acad. Sci. U. S. A. 92 (23), 10648–10652.
Sourisseau, M., Schilte, C., Casartelli, N., Trouillet, C., Guivel-Benhassine, F., Rudnicka, D., Sol-Foulon, N., Le Roux, K., Prevost, M.C., Fsihi, H., Frenkiel, M.P., Blanchet, F., Afonso, P.V., Ceccaldi, P.E., Ozden, S., Gessain, A., Schuffenecker, I., Verhasselt, B., Zamborlini, A., Saib, A., Rey, F.A., Arenzana-Seisdedos, F., Despres, P., Michault, A., Albert, M.L., Schwartz, O., 2007. Characterization of reemerging chikungunya virus. PLoS Pathog. 3 (6), e89.
Tanaka, A., Tumkosit, U., Nakamura, S., Motooka, D., Kishishita, N., Priengprom, T., Sa-Ngasang, A., Kinoshita, T., Takeda, N., Maeda, Y., 2017. Genome-wide screening uncovers the significance of n-sulfation of heparan sulfate as a host cell factor for Chikungunya virus infection. J. Virol. 91 (13).
Tani, H., Shiokawa, M., Kaname, Y., Kambara, H., Mori, Y., Abe, T., Moriishi, K., Matsuura, Y., 2010. Involvement of ceramide in the propagation of Japanese encephalitis virus. J. Virol. 84 (6), 2798–2807.
Tournebize, P., Charlin, C., Lagrange, M., 2009. [Neurological manifestations in Chikungunya: about 23 cases collected in Reunion Island]. Rev. Neurol. (Paris) 165 (1), 48–51.
Tsetsarkin, K., Higgs, S., McGee, C.E., De Lamballerie, X., Charrel, R.N., Vanlandingham, D.L., 2006. Infectious clones of Chikungunya virus (La Réunion isolate) for vector competence studies. Vector Borne Zoonotic Dis. 6 (Winter (4)), 325–337.
Umata, T., Moriyama, Y., Futai, M., Mekada, E., 1990. The cytotoxic action of diphtheria toxin and its degradation in intact Vero cells are inhibited by bafilomycin A1, a specific inhibitor of vacuolar-type H(+)-ATPase. J. Biol. Chem. 265 (35), 21940–21945.
van der Schaar, H.M., Rust, M.J., Chen, C., van der Ende-Metselaar, H., Wilschut, J., Zhuang, X., Smit, J.M., 2008. Dissecting the cell entry pathway of dengue virus by single-particle tracking in living cells. PLoS Pathog. 4 (12), e1000244.
van der Schaar, H.M., Rust, M.J., Waarts, B.L., van der Ende-Metselaar, H., Kuhn, R.J., Wilschut, J., Zhuang, X., Smit, J.M., 2007. Characterization of the early events in dengue virus cell entry by biochemical assays and single-virus tracking. J. Virol. 81 (21), 12019–12028.
Vancini, R., Wang, G., Ferreira, D., Hernandez, R., Brown, D.T., 2013. Alphavirus genome delivery occurs directly at the plasma membrane in a time- and temperature-dependent process. J. Virol. 87 (8), 4352–4359.
Voss, J.E., Vaney, M.C., Duquerroy, S., Vonrhein, C., Girard-Blanc, C., Crublet, E., Thompson, A., Bricogne, G., Rey, F.A., 2010. Glycoprotein organization of Chikungunya virus particles revealed by X-ray crystallography. Nature 468 (7324), 709–712.
Ward, B.M., 2004. Pox, dyes, and videotape: making movies of GFP-labeled vaccinia virus. Methods Mol. Biol. 269, 205–218.
Weaver, S.C., 2014. Arrival of chikungunya virus in the new world: prospects for spread and impact on public health. PLoS Negl. Trop. Dis. 8 (6), e2921.
Yoshimori, T., Yamamoto, A., Moriyama, Y., Futai, M., Tashiro, Y., 1991. Bafilomycin A1, a specific inhibitor of vacuolar-type H(+)-ATPase, inhibits acidification and protein degradation in lysosomes of cultured cells. J. Biol. Chem. 266 (26), 17707–17712.
Zhang, R., Kim, A.S., Fox, J.M., Nair, S., Basore, K., Klimstra, W.B., Rimkunas, R., Fong, R.H., Lin, H., Poddar, S., Crowe Jr, J.E., Doranz, B.J., Fremont, D.H., Diamond, M.S., 2018. Mxra8 is a receptor for multiple arthritogenic alphaviruses. Nature 557 (7706), 570–574.